

Fission dynamics study in ^{243}Am and ^{254}Fm

K. Banerjee,^{1,*} T. K. Ghosh,¹ P. Roy,¹ S. Bhattacharya,¹ A. Chaudhuri,¹ C. Bhattacharya,¹ R. Pandey,¹ S. Kundu,¹
G. Mukherjee,¹ T. K. Rana,¹ J. K. Meena,¹ G. Mohanto,² R. Dubey,² N. Saneesh,² P. Sugathan,² R. Guin,³
S. Das,³ and P. Bhattacharya⁴

¹Variable Energy Cyclotron Centre, 1/AF Bidhan Nagar, Kolkata 700 064, India

²Inter University Accelerator Centre, New Delhi 110067, India

³Radiochemistry Division, Variable Energy Cyclotron Centre, BARC, 1/AF Bidhan Nagar, Kolkata 700 064, India

⁴Saha Institute of Nuclear Physics, 1/AF Bidhan Nagar, Kolkata 700 064, India

(Received 18 September 2015; revised manuscript received 25 January 2016; published 6 June 2016)

Fission fragment mass distributions in the reactions $^{11}\text{B} + ^{232}\text{Th}$ and $^{11}\text{B} + ^{243}\text{Am}$ were measured in an energy range around the barrier. No sudden change in the width of the mass distribution as a function of center-of-mass energy was observed at near-barrier energies, indicating no quasifission transition in the near-barrier energies. Interestingly, the previous measurements of fission fragment angular anisotropies for the same systems showed significant departure from the statistical saddle-point model predictions at near-barrier energies, indicating the presence of nonequilibrium fission processes.

DOI: [10.1103/PhysRevC.93.064602](https://doi.org/10.1103/PhysRevC.93.064602)

I. INTRODUCTION

The study of fission dynamics in the actinide region has a lot of importance, as it can provide crucial information about the challenges *en route* to the formation of superheavy elements. The main hurdle to approach the super-heavy region is the quasifission process, which leads to fission before attaining full equilibration of the composite. Although theoretically the quasifission process is expected to compete with the fusion-fission process at $Z_P Z_T \gtrsim 1600$, experimental evidence of its presence is seen from $Z_P Z_T \gtrsim 750$ (Z_P and Z_T are the atomic numbers of the projectile and the target, respectively) [1,2]. In the case of quasifission, the contact configuration is more elongated than the true fission saddle-point configuration. The composite system thus formed evolves over the potential energy surface and finally overcomes the fission barrier at some conditional saddle point corresponding to a certain mass asymmetry and reaches the fission valley [3].

Several models, based on different initial conditions of the colliding nuclei, were proposed to explain the occurrence of noncompound fission processes. In the case of ground state deformed target nuclei such as actinides, the occurrence of orientation-dependent quasifission was first proposed [4]; here, the deformation of the target plays a crucial role in the fission dynamics leading to nonequilibrium fission. According to this model, as the barrier varies with orientation of the projectile-target combination, collision of the projectile with tip region of the target nucleus will lead to quasifission, whereas collision with equatorial position of the target will lead to compound nuclear fission. At sub-barrier energies, fusion predominantly takes place due to the collision of the projectile with the tip region of the deformed target nucleus. As the composite system formed after collision is more elongated compared to the saddle-point configuration, it may escape into the exit channel without being captured within the true saddle point

to form the compound nucleus, resulting in quasifission [4]. This model is successful in explaining a number of fusion reactions involving deformed actinide target nuclei, with a few exceptions, such as the $^{11}\text{B} + ^{235}\text{U}$ fusion reaction [5].

The other possible origin of quasifission may be linked to the direction of mass flow between the projectile and target in contact. According to this model, if the entrance channel mass asymmetry $\alpha = [(A_T - A_P)/(A_T + A_P)]$, A_P and A_T being the projectile and target masses, respectively] for the reaction system is smaller than the Businaro-Gallone critical mass asymmetry α_{BG} [1,5], then mass asymmetry driving force tends to act toward lower mass asymmetry, leading to dinuclear formation which evolves into a mass asymmetric saddle point, and subsequently to quasifission. Conversely, if α is greater than α_{BG} , mass flows from the lighter to the heavier side, leading to the formation of a compact mono-nucleus shape, and finally the compound nucleus. This model also explains the fusion-fission data for a wide variety of target-projectile combinations; there are, however, a few exceptions, such as $^{24}\text{Mg} + ^{178}\text{Hf}$ [6], $^{16}\text{O} + ^{194}\text{Pt}$ [7], $^{16}\text{O} + ^{197}\text{Au}$, and $^{27}\text{Al} + ^{186}\text{W}$ [8], all of which have $\alpha < \alpha_{BG}$ but did not show any signature of quasifission.

Apart from quasifission, the other significant noncompound nuclear process dominant at near-barrier energies is preequilibrium fission, which occurs if the composite system, highly fissile in general, does not attain K equilibration before fissioning (K being the projection of total angular momentum on the symmetry axis) [9]. The model of Ramamurthy and Kapoor was refined later by including the orientation-dependent effect due to target deformation [10]. The effect of nonzero spins of both target and projectile, each of which has shown to have a substantial contribution in the pre-equilibrium fission process, has been discussed by several authors [11–13].

Both quasifission and preequilibrium fission processes are operative in the same mass and energy domain and both are predicted to give rise to an anomalous fission fragment (FF) angular distribution, which was actually observed in fusion-fission studies of several heavy systems at near-barrier

*kaushik@vecc.gov.in

energies. Thus it remains a nontrivial exercise to differentiate the two processes experimentally. As far as the entrance channel dynamics is concerned, preequilibrium fission occurs before the equilibration of K degrees of freedom, whereas, in the process of quasifission, the dinuclear composite enters the fission valley bypassing the true saddle point, thus escaping the process of mass equilibration through compound nucleus formation. The presence or absence of mass equilibration, if estimated experimentally, would serve as a direct tool to differentiate between the two processes. It was already demonstrated by us in several papers (see Refs. [5,14–16] and references therein) that the width of the fragment mass distribution can be used as a measure of the degree of mass equilibration. Therefore, the fission fragment mass distribution could be a viable probe for distinguishing the two processes, when the fragment angular distribution remains ambiguous. The fission fragment mass distribution is also sensitive enough to identify other important effects such as the shell effect and the late-chance fusion fission probability [17,18].

Here we report our recent measurement of the fission fragment mass distribution in the $^{11}\text{B} + ^{232}\text{Th}$ and $^{11}\text{B} + ^{243}\text{Am}$ systems at near- and below-barrier energies. Both the target nuclei are deformed in their ground state (^{232}Th : $\beta_2 = 0.207$; ^{243}Am : $\beta_2 = 0.224$). So, one would expect to observe noncompound fission in both systems, provided the orientation-dependent entrance channel dynamics is the only (most dominant) factor deciding the evolutionary process of fusion (quasifission). On the other hand, if the entrance channel mass asymmetry is the key parameter controlling the dynamics, then we should not expect any occurrence of a noncompound fission process in any of the two systems, as the entrance channel mass asymmetry for both systems is higher than the respective Businaro-Gallone critical mass asymmetry (for $^{11}\text{B} + ^{232}\text{Th}$, α is 0.909, α_{BG} is 0.886; for $^{11}\text{B} + ^{243}\text{Am}$, α is 0.913, α_{BG} is 0.903). Two previous measurements on angular distribution for the present systems are available in the literature [13,19], by the reported fragment angular anisotropy $A [=W(0^\circ)/W(90^\circ)]$, where $W(0^\circ)$ and $W(90^\circ)$ are the fragment yields at 0° (or equivalently 180°) and 90° with respect to the beam axis] for both the systems was found to be significantly larger than the corresponding statistical saddle-point model (SSPM) prediction at sub-barrier energies. This indicates the presence of a nonequilibrium fission process in both reactions. The aim of the present work is to explore further into the nature of the nonequilibrium fission (pre-equilibrium fission and/or quasifission) process in these systems by studying the systematic variation of the width of the fragment mass distribution, which has already been demonstrated to be an unambiguous probe to identify quasifission.

II. EXPERIMENTAL DETAILS

The experiment was performed using a pulsed beam of ^{11}B obtained from the 15UD Pelletron accelerator at the Inter University Accelerator Centre (IUAC), New Delhi. The targets used were self-supporting ^{232}Th of 1.1 mg/cm^2 thickness and ^{243}Am of $80 \text{ } \mu\text{g/cm}^2$ thickness, electrodeposited on ^{27}Al backing of $200 \text{ } \mu\text{g/cm}^2$ thickness. The measurements were

carried out at $E_{\text{lab}} = 56, 59, 61, 63, 66, 70,$ and 74 MeV . For the detection of fission fragments, two large-area ($20 \text{ cm} \times 6 \text{ cm}$) position sensitive multi wire proportional counters (MWPCs) were placed at the folding angle for symmetric fission, at distances of 36.5 and 50 cm, from the center of the target on either side of the beam axis. Beam flux monitoring as well as normalization were done using the elastic events collected by two silicon surface barrier detectors placed at $\pm 10^\circ$. The event collection was triggered by the detection of a fission fragment in any of the MWPC detectors.

III. DATA ANALYSIS

It is well known that, at bombarding energy close to the Coulomb barrier, transfer fission (TF) is a dominant reaction channel. So, in order to extract the contributions of compound fission and noncompound fission (quasifission, preequilibrium fission), both of which are full momentum transfer processes, the TF contribution needs to be separated from experimental data [20]. The fission fragments from full momentum transfer events were exclusively selected from the correlation of the velocity of the fissioning system (v_{\parallel}) in the beam direction relative to the recoil of the fused system and the velocity perpendicular to the reaction plane (v_{\perp}) [21], as well as the correlation of the polar and azimuthal angles of the fragment (θ, ϕ) with respect to the beam axis. Figure 1 displays a typical fragment velocity distribution measured at $E_{\text{lab}} = 61 \text{ MeV}$. For the fusion-fission process, the events were centered around the velocity coordinates $((v_{\parallel} - v_{CN}), v_{\perp}) = (0, 0)$. The events corresponding to TF are scattered around nonzero $((v_{\parallel} - v_{CN}), v_{\perp})$ values.

The polar folding angle distribution is shown in Fig. 2, which shows that the measured folding angle distribution of FF events is peaked around 166° , consistent with the expected value for full momentum transfer (FMT) events. The arrow

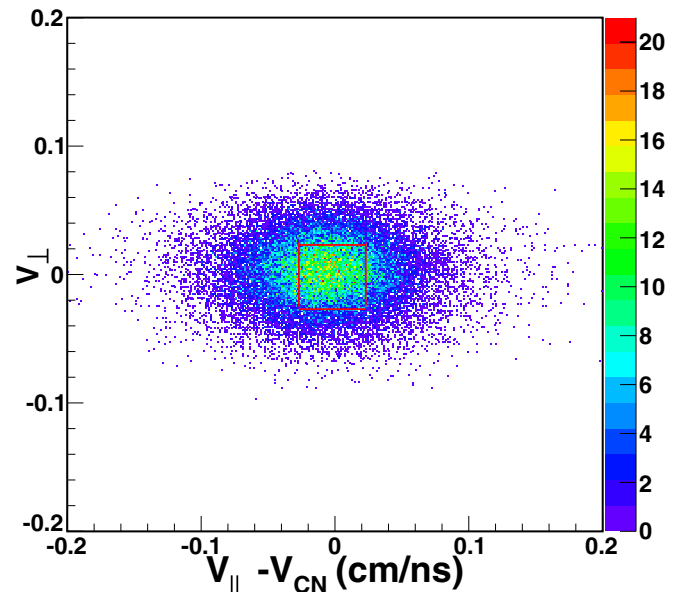


FIG. 1. Measured distribution of velocity of the fissioning nuclei in the reaction $^{11}\text{B} + ^{232}\text{Th}$ at $E_{\text{lab}} = 61 \text{ MeV}$. The (red) rectangle indicates the gate used to select the FF events for mass determination

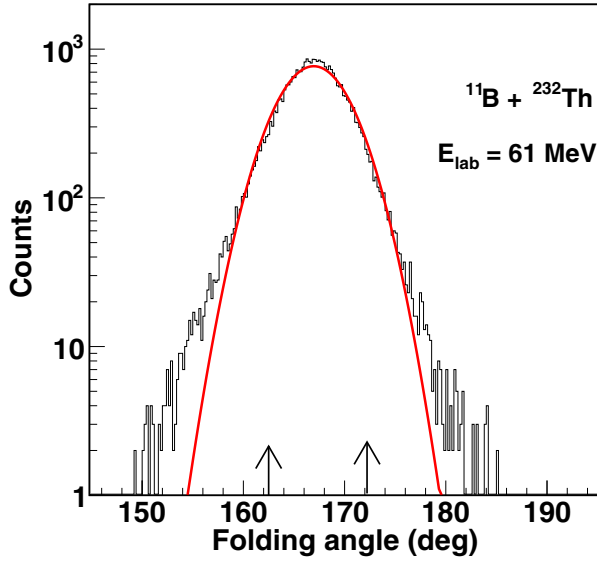


FIG. 2. Measured folding angle distribution of all fission fragments in the reaction $^{11}\text{B} + ^{232}\text{Th}$ at $E_{\text{lab}} = 61$ MeV. The two arrows indicate the gate used to select the FF events for mass determination.

used in the figure is to show the gate considered for the extraction of the fission fragments mass. The fission fragments are well separated from elastic and quasielastic reaction channels, as far as the time correlation and energy loss spectra are concerned. The fragment masses were determined from the difference of the time of flight, polar and azimuthal angles, and momentum and recoil velocities for each event [22], after incorporating appropriate correction in the data to take care of the effect of energy loss and straggling of the fission fragment due to finite thickness of the target and backing materials [23].

IV. RESULTS AND DISCUSSIONS

The extracted fission fragment mass distributions near and above the coulomb barrier energies are shown in Fig. 3 for the $^{11}\text{B} + ^{232}\text{Th}$ system and in Fig. 4 for the $^{11}\text{B} + ^{243}\text{Am}$ system. It is observed that the measured mass distributions are well fitted with a single Gaussian distribution at all energies. The variation of the standard deviation (σ_m) of the fitted Gaussian distribution as a function of $E_{c.m.}/V_b$, where $E_{c.m.}$ is the incident energy in center of mass and V_b the Coulomb barrier, is shown in Fig. 5. From the figure it is evident that the width of the mass distribution as a function of $E_{c.m.}/V_b$ is monotonic in nature; there is no significant departure from the continuous nature of variation of the width of the mass distribution at below-barrier energies in the $^{11}\text{B} + ^{232}\text{Th}$ and $^{11}\text{B} + ^{243}\text{Am}$ systems. The absence of any abrupt change in the width of the mass distribution at below-barrier energies signifies that the degree of mass equilibration underwent no sudden change over the whole energy range under consideration. We can reasonably argue that, in both cases presented here, fission occurred from mass-equilibrated composite. In other words, the possibility of quasifission, if not ruled out, may not be significant in both cases in the measured energy range, in spite of the fact that both systems had large target deformation which

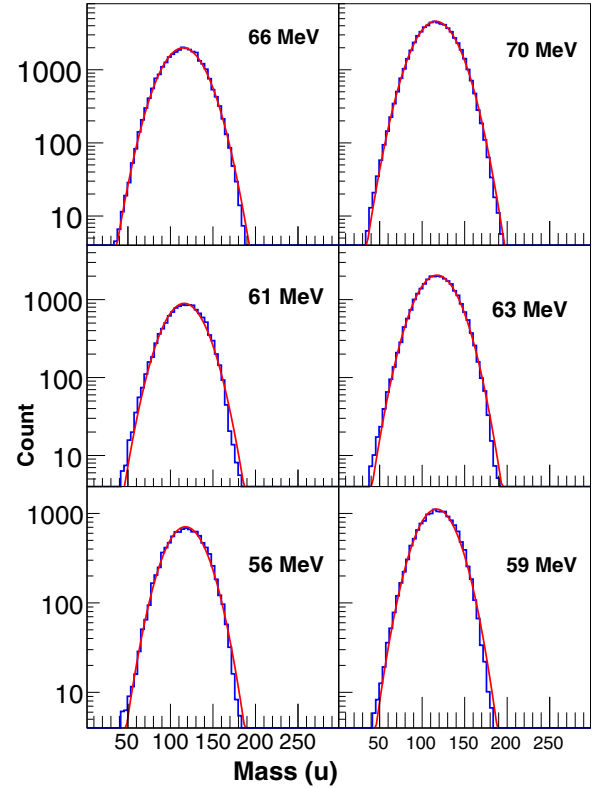


FIG. 3. Measured mass distributions (blue histogram) for the reactions $^{11}\text{B} + ^{232}\text{Th}$ at different laboratory energies. The Gaussian fits are shown by (red) solid lines

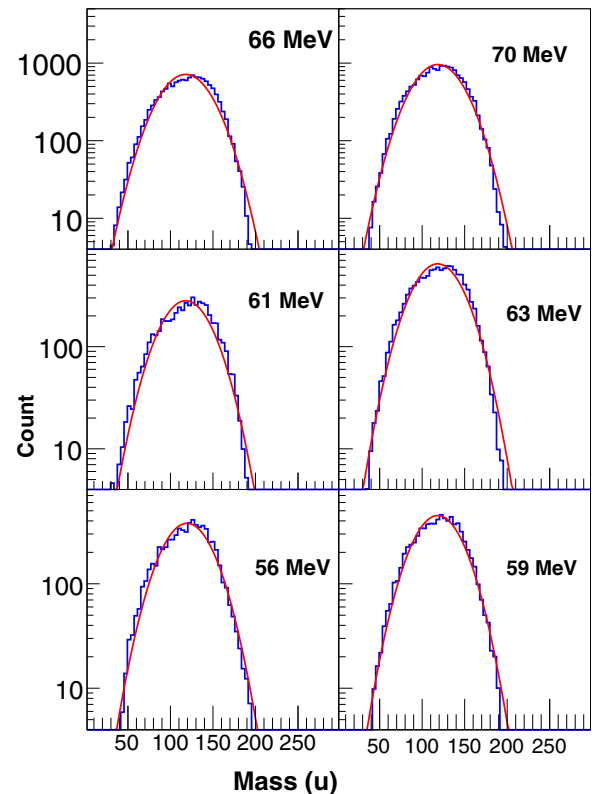


FIG. 4. Same as Fig. 3 for the $^{11}\text{B} + ^{243}\text{Am}$ system

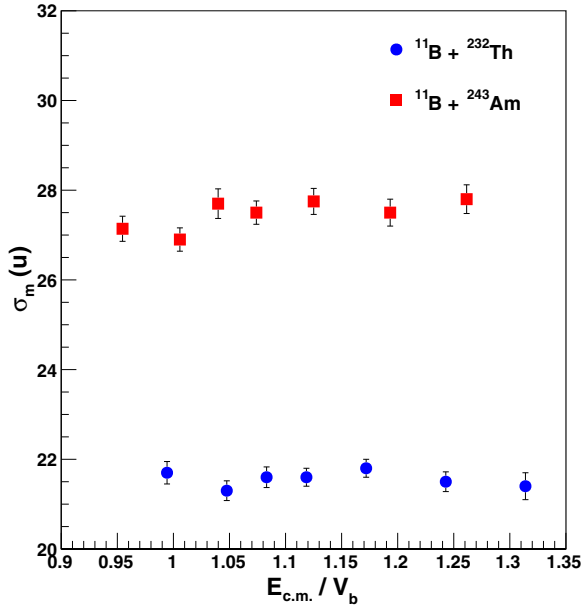


FIG. 5. Variation of the σ_m as a function of $E_{c.m.}/V_b$.

could have triggered orientation-dependent quasifission, as seen in several such cases. On the other hand, for both systems, the entrance channel mass asymmetry α was greater than α_{BG} , thereby preferring the mass flow toward the direction of higher asymmetry, leading to mononucleus formation to end up as compound nucleus. In the present case, the mechanism of mass flow seems to be stronger enough to overcome the orientation-dependent quasifission mechanism to drive the system toward mass equilibration and fusion. That the direction of mass flow decides the entrance channel dynamics is further apparent if the present mass distribution result for the $^{11}\text{B} + ^{243}\text{Am}$ system is compared with that obtained earlier for the $^{16}\text{O} + ^{238}\text{U}$ system [15]; both the systems produce the same compound system ^{254}Fm , but the value of α was greater than α_{BG} in the former, and less than α_{BG} in the latter. Therefore, one should have observed the signature of quasifission in the latter case. A sudden variation in the width of the mass distribution at near-barrier energies was reported in the $^{16}\text{O} + ^{238}\text{U}$ system, which indicates non-equilibration of mass asymmetry. This is a conclusive evidence of quasifission transition at near-barrier energies. Fission fragment angular anisotropy and mass distribution were also measured by Hinde *et al.*, confirming the quasifission transition at around barrier energies [21]. This finding, however, also supports the orientation effect in the quasifission transition in the $^{16}\text{O} + ^{238}\text{U}$ system.

The orientation effect in fission dynamics can be further visualized through the study [24] of driving potential as a function of mass asymmetry; Fig. 6 shows the entrance channel potential energy as a function of mass asymmetry, calculated using the proximity potential with two-center shell model deformation energy [25]. The entrance channel mass asymmetry of both the systems is higher than their respective α_{BG} . From the figure it is evident that the system prefers to move toward higher mass asymmetry for both orientations,

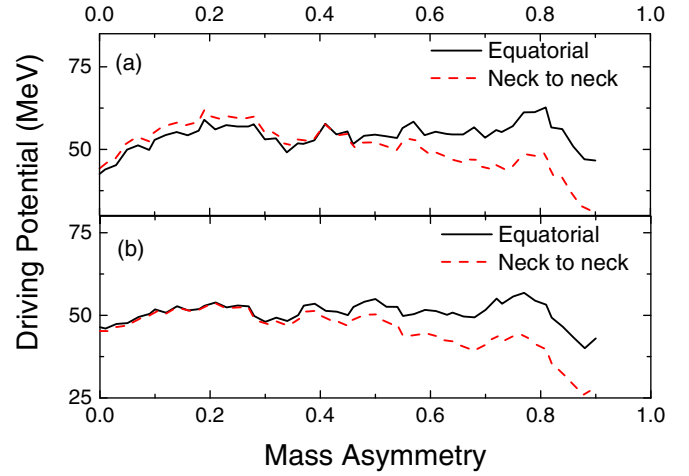


FIG. 6. Driving potential at the contact configuration as a function of mass asymmetry for two different orientations of the deformed target nucleus: (a) $^{11}\text{B} + ^{243}\text{Am}$ system, (b) $^{11}\text{B} + ^{232}\text{Th}$ system.

which is toward the compound nucleus formation. In other words no quasifission transition is expected in either of the two systems for both entrance channel asymmetry as well as orientation points of view.

It is now tempting, keeping the two results of fragment mass distribution and angular anisotropy side by side, to arrive at a conclusion about the nature of the fission dynamics route followed in the cases of $^{11}\text{B} + ^{232}\text{Th}$ and $^{11}\text{B} + ^{243}\text{Am}$. It is clear that none of them followed the quasifission route as there was no sign of transition to quasifission in the below-barrier energy domain as far as the width of the mass distribution is concerned; thus the observed anisotropy in fission fragment angular distribution should only be due to the predominance of the other alternative, i.e., preequilibrium fission in both cases.

It may be pointed out here that preequilibrium fission is also strongly influenced by both entrance channel deformation [10], spin [13], and asymmetry [26]. Orientation-dependent quasifission due to entrance channel deformation is ruled out by the present measurement. However, the occurrence of preequilibrium fission due to the orientation effect may not be ruled out, as anomalous angular anisotropy was seen in both cases. Conversely, both the systems have $\alpha > \alpha_{BG}$, which excluded the possibility of occurrence of quasifission as well as the preequilibrium fission in these systems [26]. So, we arrive at an interesting juncture; as far as quasifission is concerned the present mass distribution results indicate that the entrance channel mass asymmetry, and not the deformation of the target, decides the fusion route. On the other hand, angular anisotropy results indicate the opposite: it is the orientation effect due to deformation, and not the entrance channel mass asymmetry, which decides when nonequilibrium fission (here it is preequilibrium fission only, as quasifission has already been ruled out) will occur. This clearly points to gaps in our present understanding of the nonequilibrium fission phenomenon, which is essentially phenomenological in nature. A detailed microscopic study to chart the entrance channel dynamics using realistic multidimensional potential energy surfaces is required to have a clear understanding of the

distinctive features of relaxation of various degrees of freedom at near-barrier region.

V. SUMMARY AND CONCLUSIONS

The present study confirms that the anomalous angular anisotropy observed in $^{11}\text{B} + ^{232}\text{Th}$ and $^{11}\text{B} + ^{243}\text{Am}$ at near barrier energies is not due to quasifission, as the mass distribution data do not display any signature of transition to quasifission at near-barrier energies. Therefore, it is concluded that the anisotropy observed in the angular distribution in previous measurements might only be due to the presence of a preequilibrium fission process. It was also observed that either of the two important factors decide the entrance channel dynamics; i.e., the mutual orientation of the projectile with respect to the deformed target nucleus and the entrance channel mass asymmetry. From the present data, it seems

that the quasifission possibility was decided mainly by the entrance channel mass asymmetry, whereas the occurrence of preequilibrium fission is seems to be decided by the orientation of the projectile with respect to the deformed target nucleus. It will be interesting to understand the relative importance of interplay of various processes through proper microscopic understanding of the relaxation of relevant degrees of freedom.

ACKNOWLEDGMENTS

The authors are thankful to the IUAC Pelletron staff for providing high quality pulsed beams for the experiment. An illuminating discussion with Jhiliam Sadhukhan is thankfully acknowledged. One of the authors (S.B.) acknowledges with thanks financial support received from the Department of Atomic Energy, Government of India.

-
- [1] A. C. Berriman *et al.*, *Nature (London)* **413**, 144, (2001).
- [2] E. Williams, D. J. Hinde, M. Dasgupta, R. du Rietz, I. P. Carter, M. Evers, D. H. Luong, S. D. McNeil, D. C. Rafferty, K. Ramachandran, and A. Wakhle, *Phys. Rev. C* **88**, 034611 (2013).
- [3] W. J. Swiatecki, *Phys. Scr.* **24**, 113 (1981).
- [4] D. J. Hinde, M. Dasgupta, J. R. Leigh, J. P. Lestone, J. C. Mein, C. R. Morton, J. O. Newton, and H. Timmers, *Phys. Rev. Lett.* **74**, 1295 (1995).
- [5] T. K. Ghosh, K. Banerjee, C. Bhattacharya, S. Bhattacharya, S. Kundu, P. Mali, J. K. Meena, G. Mukherjee, S. Mukhopadhyay, T. K. Rana, P. Bhattacharya, and K. S. Golda, *Phys. Rev. C* **79**, 054607 (2009).
- [6] R. Rafiei, R. G. Thomas, D. J. Hinde, M. Dasgupta, C. R. Morton, L. R. Gasques, M. L. Brown, and M. D. Rodriguez, *Phys. Rev. C* **77**, 024606 (2008).
- [7] E. Prasad, K. M. Varier, R. G. Thomas, P. Sugathan, A. Jhingan, N. Madhavan, B. R. S. Babu, R. Sandal, S. Kalkal, S. Appannababu, J. Gehlot, K. S. Golda, S. Nath, A. M. Vinodkumar, B. P. Ajithkumar, B. V. John, G. Mohanto, M. M. Musthafa, R. Singh, A. K. Sinha, and S. Kailas, *Phys. Rev. C* **81**, 054608 (2010).
- [8] S. Appannababu, S. Mukherjee, B. K. Nayak, R. G. Thomas, P. Sugathan, A. Jhingan, E. Prasad, D. Negi, N. N. Deshmukh, P. K. Rath, N. L. Singh, and R. K. Choudhury, *Phys. Rev. C* **83**, 034605 (2011).
- [9] V. S. Ramamurthy and S. S. Kapoor, *Phys. Rev. Lett.* **54**, 178 (1985).
- [10] D. Vorkapic and B. Ivanisevic, *Phys. Rev. C* **52**, 1980 (1995).
- [11] R. D. Butt, D. J. Hinde, M. Dasgupta, A. C. Berriman, A. Mukherjee, C. R. Morton, and J. O. Newton, *Phys. Rev. C* **66**, 044601 (2002).
- [12] J. P. Lestone, A. A. Sonzogni, M. P. Kelly, and R. Vandenbosch, *Phys. Rev. C* **56**, R2907(R) (1997).
- [13] B. K. Nayak *et al.*, *Phys. Rev. C* **62**, 031601 (2000).
- [14] T. K. Ghosh, S. Pal, T. Sinha, S. Chattopadhyay, P. Bhattacharya, D. C. Biswas, and K. S. Golda, *Phys. Rev. C* **70**, 011604(R) (2004).
- [15] K. Banerjee, T. K. Ghosh, S. Bhattacharya, C. Bhattacharya, S. Kundu, T. K. Rana, G. Mukherjee, J. K. Meena, J. Sadhukhan, S. Pal, P. Bhattacharya, K. S. Golda, P. Sugathan, and R. P. Singh, *Phys. Rev. C* **83**, 024605 (2011).
- [16] A. Chaudhuri, T. K. Ghosh, K. Banerjee, S. Bhattacharya, Jhiliam Sadhukhan, C. Bhattacharya, S. Kundu, J. K. Meena, G. Mukherjee, R. Pandey, T. K. Rana, P. Roy, T. Roy, V. Srivastava, and P. Bhattacharya, *Phys. Rev. C* **91**, 044620 (2015).
- [17] M. Caamaño, O. Delaune, F. Farget, X. Derckx, K.-H. Schmidt, L. Audouin, C. O. Bacri, G. Barreau, J. Benlliure, E. Casarejos, A. Chbihi, B. Fernández-Dominguez, L. Gaudefroy, C. Golabek, B. Jurado, A. Lemasson, A. Navin, M. Rejmund, T. Roger, A. Shrivastava, and C. Schmitt, *Phys. Rev. C* **88**, 024605 (2013).
- [18] J. Khuyagbaatar, D. J. Hinde, I. P. Carter, M. Dasgupta, C. E. Düllmann, M. Evers, D. H. Luong, R. duRietz, A. Wakhle, E. Williams, and A. Yakushev, *Phys. Rev. C* **91**, 054608 (2015).
- [19] R. Tripathi, K. Sudarshan, S. Sodaye, S. K. Sharma, and A. V. R. Reddy, *Phys. Rev. C* **75**, 024609 (2007).
- [20] N. Majumdar, P. Bhattacharya, D. C. Biswas, R. K. Choudhury, D. M. Nadkarni, and A. Saxena, *Phys. Rev. C* **51**, 3109 (1995).
- [21] D. J. Hinde, M. Dasgupta, J. R. Leigh, J. C. Mein, C. R. Morton, J. O. Newton, and H. Timmers, *Phys. Rev. C* **53**, 1290 (1996).
- [22] T. K. Ghosh, S. Pal, T. Sinha, S. Chattopadhyay, K. S. Golda, and P. Bhattacharya, *Nucl. Instrum. Methods Phys. Res. A* **540**, 285 (2005).
- [23] M. N. Rao, D. C. Biswas, and R. K. Choudhury, *Nucl. Instrum. Methods Phys. Res. B* **51**, 102 (1990).
- [24] D. J. Hinde, R. G. Thomas, R. duRietz, A. Diaz-Torres, M. Dasgupta, M. L. Brown, M. Evers, L. R. Gasques, R. Rafiei, and M. D. Rodriguez, *Phys. Rev. Lett.* **100**, 202701 (2008).
- [25] V. Zagrebaev *et al.*, *Phys. Part. Nucl.* **38**, 469 (2007), NRV code for driving potential, <http://nrv.jinr.ru/nrv/>
- [26] V. S. Ramamurthy, S. S. Kapoor, R. K. Choudhury, A. Saxena, D. M. Nadkarni, A. K. Mohanty, B. K. Nayak, S. V. Sastry, S. Kailas, A. Chatterjee, P. Singh, and A. Navin, *Phys. Rev. Lett.* **65**, 25 (1990).